

# 次世代のジェットエンジンのタービン翼に向けた亀裂自己治療可能を有するハイブリッド材料の新しいコンセプト

グエン タン ソン\*, 高橋 剛\*

## New Concept of Hybrid Materials with Permanent Self-Crack Healing Ability for Next Generation of Jet-Engine Turbine Blades

Son Thanh NGUYEN , Tsuyoshi TAKAHASHI

In gas turbine engine, environmental barrier coatings (EBCs) are used protect the SiC/SiC ceramic blades against hot steam, the main cause for SiC evaporation. The topcoat layer of EBC is easy to be cracked by foreign objects, thus self-crack healing ability is necessary. This layer can be reinforced with a healing agent material, which reacts with oxygen during operation to produce molten glass that can flow into and seal the cracks. In this paper, we introduce  $\text{Yb}_2\text{Si}_2\text{O}_7$ - $\text{Yb}_2\text{SiO}_5$ -SiC as a candidate for the topcoat, then propose a special process to permanently retain the self-crack healing ability for this hybrid material.

Key word: self-crack healing, strength, hybrid materials, turbine blades, SiC

### 1. Introduction

In these years, aviation industry is developing at remarkable speed that require improvements in the fuel efficiency of gas turbine engine [1]. Until 2025, the operation temperature of the turbine is expected to reach 1500 °C, and SiC/SiC composite has been proposed as the material for engine's turbine blade [2]. However, since SiC is very likely to be evaporated in water vapor environment, it is necessary to coat the surface of the blade with environmental-barrier-coating layers (EBCs) to shield it from hot steam [3]. The fracture toughness of the topcoat ceramics in EBC is quite low, thus it is necessary to improve this property to avoid the failure when the blades colliding with foreign objects during operation. As illustrated in Fig. 1,

ceramics with self-crack healing ability are being studied as a solution for this problem. Conventionally, self-crack healing ceramics are reinforced with healing agents such as SiC, Ni nanoparticles, which turn to oxide in reaction with oxygen at high temperature, then this molten oxide flow into the cracks and seal them [4–6]. However, once the all dispersed nanoparticles turned to oxide, self-crack healing ability can no longer be available. For the long service life-time of the gas turbine, it is important to use this self-healing process repeatedly, but there still have been no coating materials that can permanently retain the self-crack healing ability.

Recently, the authors successfully demonstrated the self-crack healing ability on the surface of  $\text{Yb}_2\text{Si}_2\text{O}_7$  -  $\text{Yb}_2\text{SiO}_5$  - SiC (YYs), a promising hybrid

---

\* 釧路高専創造工学科 機械工学分野

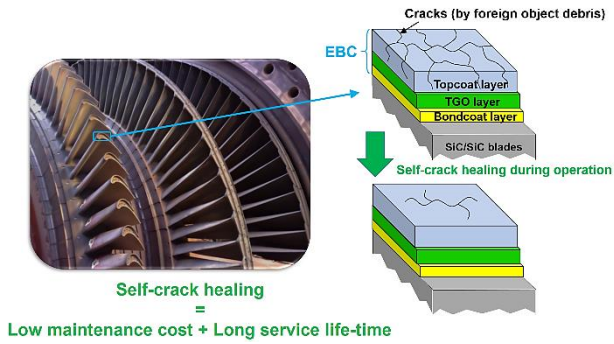


Fig. 1 Schematic illustration for self-crack healing EBC

material for the EBC topcoat [7]. In this hybrid, monosilicate  $\text{Yb}_2\text{SiO}_5$  reacted with  $\text{SiO}_2$  to form disilicate  $\text{Yb}_2\text{Si}_2\text{O}_7$ , which volume expansion helped to seal the crack. Interestingly, the strength of hybrid not only recovered to the virgin value, but also increased around 20% due to the residual compressive stress at healed-crack sites.

On the other hand, it was reported that  $\text{Yb}_2\text{Si}_2\text{O}_7$  can be decomposed to  $\text{Yb}_2\text{SiO}_5$  and  $\text{Si}(\text{OH})_4$  when being heated in water vapor in the range of 1300 ~ 1400 °C [8]. Therefore, if the heating process is optimized, it is reasonable to expect that a recycle – reuse process of  $\text{Yb}_2\text{SiO}_5$  can be employed to permanently provide the hybrid with crack-healing ability (see Fig. 2). In other words, we can develop the first permanent self-crack healing hybrid material in the world, that would be very beneficial for the next generation of gas turbine.

The objective of this research project is to synthesize permanent self-crack healing hybrid materials by using a special heat treatment process, in which the healing agent is continuously recovered. As a result, we can expect to the increase of the fuel efficiency of the next-generation of gas turbine.

In the present paper, we introduce YYS as a self-crack-healing hybrid material for EBC, as well as explain its healing mechanism. Then, we report the first results of the research project fabricating permanent self-crack healing materials.

## 2. Experimental Procedures

### 2.1. Starting materials and the synthesis of the hybrid

The hybrid was synthesized by solid state reaction and hot-pressing method.  $\text{Yb}_2\text{O}_3$  (99.9%, Shin-Etsu Chemical, Japan) and  $\text{SiO}_2$  (99.5%, Sigma

Aldrich, USA) powders were first mixed in 1:2 molar ratio, then a corresponding volume fraction (0 ~ 20 vol.%) of cubic SiC nanopowder (IBIDEN, Japan) was added to produce a powder mixture. The mixture was then ball-milled in high purity ethanol overnight, followed by evaporation and drying at 80°C for 24 h. Afterwards, the mixture was dry ball-milled and then sieved to break up agglomerates. Next, this prepared fine powder mixture was hot-pressed in a sintering furnace (FVPHP-R-5, FRET-18, Fuji Dempa Kogyo, Japan) at 30 MPa, 1550 °C for 1 h, in argon (Ar) gas to obtain sintered disks (44 mm-diameter).

### 2.2. Measurements and analyses

For bending strength measurement, the sintered disks were cut into rectangular specimens (36 mm × 4 mm × 3 mm), then their long edges were beveled at 45°, according to JIS R1601. Bending strength of the hybrids was measured at room temperature by four-point bending method using a testing system (MODEL-1311 VRW, Aikoh Engineering, Japan). The outer span  $L$  and inner span  $l$  were 30 and 10 mm, and the crosshead speed was set at 0.5 mm/min. The bending strength  $\sigma_B$  of a specimen is given by the following equation:

$$\sigma_B = \frac{3P(L-l)}{2wt^2} \quad (1)$$

where  $w$  and  $t$  are the width and thickness of the specimen, and  $P$  is the load when the specimen is broken. To investigate the impact of surface cracks on the bending strength, on the surface of specimens, cracks were prepared by using a Vickers hardness tester (HV-100, Mitutoyo, Japan) with 2 kgf indentation load. The as-indented specimens were annealed in at 1250 °C for 2 h to activate their crack-healing ability.



Fig. 2 Concept of recycle – reuse process for permanent self-crack healing ability

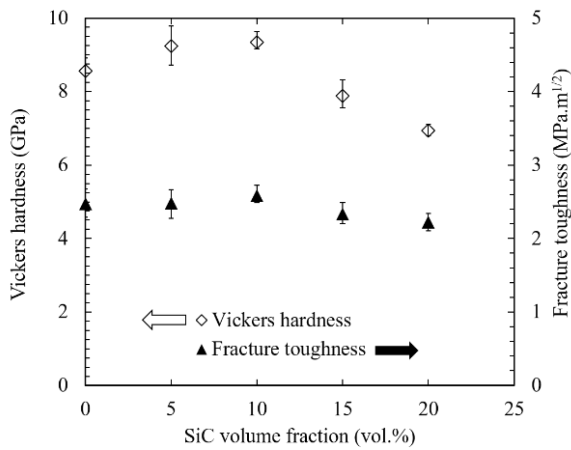


Fig. 3 Vickers hardness and fracture toughness of sintered hybrids

The cross-sections of specimens and the cracks induced by Vickers indenters were observed using a tabletop scanning electron microscope (SEM) TM-3000 (Hitachi High-Technologies, Japan). Vickers hardness  $H_V$  and fracture toughness  $K_{Ic}$  were calculated using following equations [9]:

$$H_V = 1.854F/d^2 \quad (2)$$

$$K_{Ic} = 0.203H_V a^2 c^{-1.5} \quad (3)$$

where  $F$  is the indentation load,  $d$  is the indentation diagonal length,  $a$  is the half-diagonal length, and  $c$  is the half-crack length.

Crystalline phases of synthesized powder mixture and sintered hybrids were identified using an X-ray diffractometer (XRD, RINT 2500PC, Rigaku, Japan) with Cu-K $\alpha$  radiation ( $\lambda = 1.54186 \text{ \AA}$ ). The scan range was  $20 - 70^\circ$  and step angle was  $0.02^\circ$ . High resolution micrographs of indentation cracks were obtained with a field emission scanning electron microscope (FE-SEM; JSM-7001 FA, Jeol, Japan). The identity of healing agents was investigated using an attached energy-dispersive X-ray spectrometer (EDS). To avoid the charge-up effect during observation, samples were coated with a thin conductive layer ( $\sim 5 \text{ nm}$ ) using a JFC-1600 Fine Coater (Jeol, Japan)

### 2.3. Recycling $\text{Yb}_2\text{SiO}_5$ by thermal treatment

Annealed hybrids were then thermally treated in a specific water vapor furnace (Japan Fine Ceramics Center, Japan) at  $800^\circ\text{C}$  for 1 h. The flow rate of water vapor was  $5\text{kg/h}$ , both heating and cooling rates were  $10^\circ\text{C/min}$ . After the thermal treatment, sample was brought to composition analysis to confirm whether the decomposition of  $\text{Yb}_2\text{Si}_2\text{O}_7$  to

$\text{Yb}_2\text{SiO}_5$  and  $\text{Si}(\text{OH})_4$  occurred at this heat treating condition.

## 3. Results

The measurement results of Vickers hardness and fracture toughness were summarized in Fig. 3. Vickers hardness of the hybrid without SiC reinforcement (hereafter, called as ytterbium silicates) is  $8.5 \text{ GPa}$  for  $2 \text{ kgf}$  indentation load. The reinforcement with SiC should increase the hardness. Indeed, the hardness increased with SiC content and reached a maximum value of  $9.3 \text{ GPa}$  at  $10 \text{ vol.}\%$  SiC. However, the hardness of hybrids decreased noticeably with further increase of SiC content. The hardness of the hybrid dispersed with  $20 \text{ vol.}\%$  SiC is  $6.9 \text{ GPa}$ , which is only  $80\%$  of the value of ytterbium silicates. The fracture toughness of the ytterbium silicates is  $2.5 \text{ MPa.m}^{1/2}$ , which falls between that of monosilicate ( $2.3 \text{ MPa.m}^{1/2}$ ) and

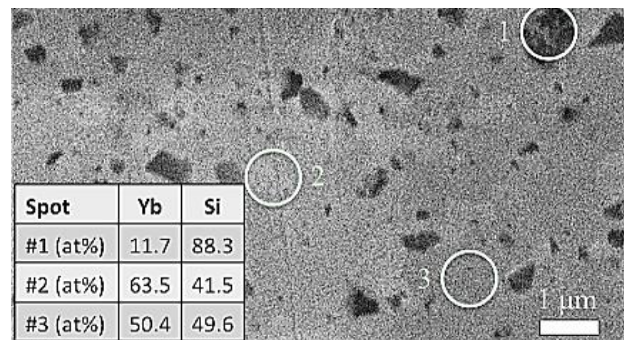
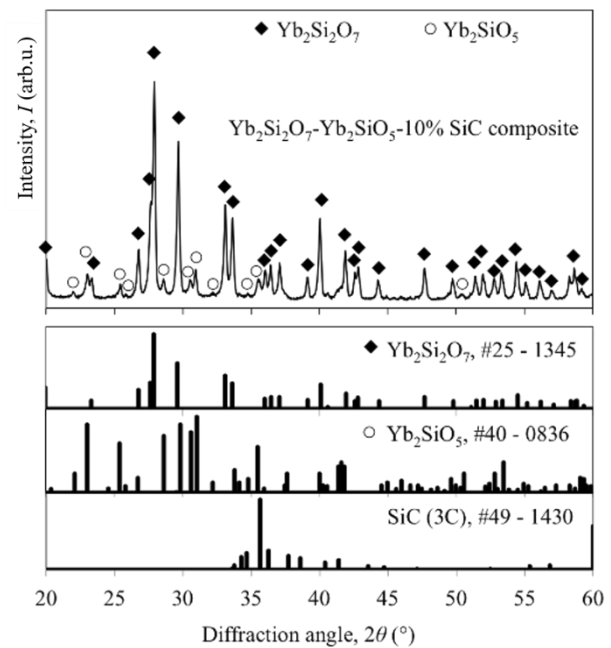


Fig. 4 XRD pattern (top) and SEM-EDS analysis (bottom) of the surface of hybrid dispersed with  $10 \text{ vol.}\%$  SiC

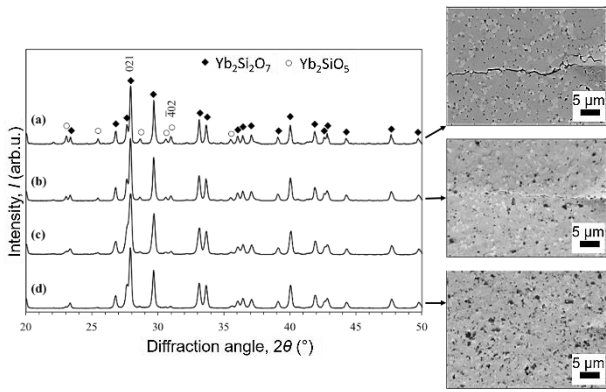


Fig. 5 XRD patterns of hybrids with (a) 0 vol.% SiC; (b) 5 vol.% SiC; (c) 10 vol.% SiC; (d) 20 vol.% SiC after annealing and their indentation cracks observed by SEM

disilicate ( $2.7 \text{ MPa}\cdot\text{m}^{1/2}$ )[10]. The fracture toughness  $K_{Ic}$  of hybrids varied similarly to hardness. The toughness first slightly increased but started to decrease when SiC content higher than 10 vol.%. The coexistence of three independent phases is considered as the main reason for the low density of hybrids with high SiC content, resulting in the deterioration of hardness and toughness.

Figure 4a shows the XRD pattern of 10 vol.% SiC hybrid before annealing, and Fig. 4b is the SEM-EDS composition analysis of the hybrid. Both  $\text{Yb}_2\text{Si}_2\text{O}_7$  and  $\text{Yb}_2\text{SiO}_5$  diffraction peaks appear, indicating the co-existence of the two silicates in the hybrid. It is very difficult to identify SiC using XRD patterns because the SiC volume fraction is very small and most of SiC diffraction peaks are overlapped by  $\text{Yb}_2\text{Si}_2\text{O}_7$  and  $\text{Yb}_2\text{SiO}_5$  peaks. Figure 4b shows three distinct domains (black, light gray, and dark gray) in the surface of hybrids. EDS analysis of revealed that Si prevails in black domains (site #1) with Yb:Si = 11.7:88.3, suggesting that they are silicon carbide particles. The atomic ratio Yb:Si in light gray domains (site #2) is  $63.5:41.5 = 1.7$ , suggesting that light gray domains are  $\text{Yb}_2\text{SiO}_5$ . In dark gray domains (site #3), the ratio Yb:Si is  $50.4:49.6 \approx 1$ , indicating these domains are  $\text{Yb}_2\text{Si}_2\text{O}_7$ . Then we applied a photographic analyzing technique to calculate the surface area fraction of SiC (black domains) and estimated that volume fraction of silicon carbide is 10.7 %. This result is in consistent with the volume fraction of silicon carbide (10 vol.%) in the powder mixture of the hybrid,

confirming that SiC did not react with the silicates during sintering.

Figure 5 shows the XRD patterns and the SEM observation of hybrids after annealing in air at  $1250^\circ\text{C}$  for 2 h. Figure 6 shows XRD patterns and SEM observation of hybrid with 10 vol.% SiC, before and after annealing in air or Ar. For hybrid with 5 vol.% SiC (Fig. 5b), the cracks were partly healed after annealing. After annealing, the diffraction peak intensity of  $\text{Yb}_2\text{SiO}_5$  became lower, indicating the  $\text{Yb}_2\text{SiO}_5$  fraction in the hybrid decreased. Regarding hybrid with 10 vol.% SiC, the cracks almost disappeared after annealing in air (Figs. 5a and b). In addition, the  $\text{Yb}_2\text{SiO}_5$  diffraction peak intensity in the hybrid also decreased (Fig. 5c). However, the crack length and XRD peak intensity almost did not change when annealing the hybrid in Ar (Figs. 6a and 6c), indicating that the annealing in inert gas had very limited effect on crack healing. In hybrid with 20 vol.% SiC, the cracks were almost fully healed by annealing in air, and  $\text{Yb}_2\text{SiO}_5$  almost disappeared from the surface (Fig. 5d).

## 4. Discussion

### 4.1. Self-crack healing mechanism

Figure 7 shows the schematic illustration of the self-crack healing process in the hybrids. SiC nanoparticles were dispersed homogeneously in the hybrid, either in the grains or on the grain boundaries of  $\text{Yb}_2\text{Si}_2\text{O}_7$  or  $\text{Yb}_2\text{SiO}_5$ . When an indentation load is applied on the hybrid surface, cracks develop from the corners of indentation and propagate through some silicate grains and SiC particles, resulting in

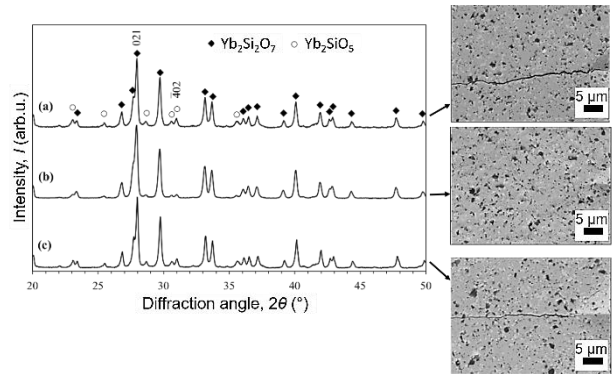


Fig. 6 XRD patterns of hybrids with 10 vol.% SiC: (a) before annealing; (b) after annealing in air; (c) after annealing in Ar; and their indentation cracks observed by SEM

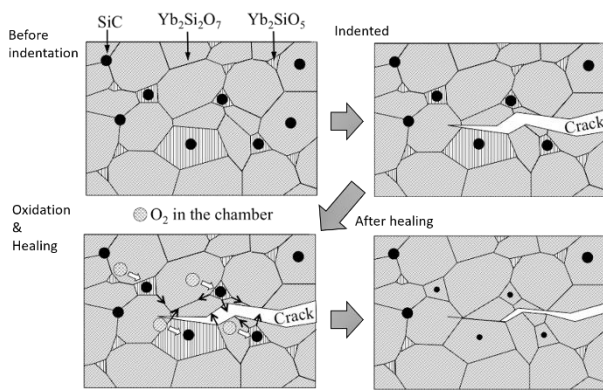
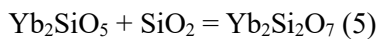


Fig. 7 Schematic illustration for self-crack healing in YYS hybrids

defects on the surface of hybrid. When the hybrid is annealed in air atmosphere, SiC particles at the surface are oxidized and form  $\text{SiO}_2$  glass as follows:  $\text{SiC}_{(s)} + 2\text{O}_{2(g)} = \text{SiO}_{2(s)} + \text{CO}_{2(g)} + 943 \text{ kJ/mol}$  (4)

The annealing temperature here is  $950 \sim 1400 \text{ }^\circ\text{C}$ , lower than the melting point of  $\text{SiO}_2$  ( $1650 \text{ }^\circ\text{C}$ ), the great heat ( $943 \text{ kJ/mol}$ ) generated from this strong exothermic reaction, can raise the local temperature at the reacting sites an increment of  $400 \text{ }^\circ\text{C}$  [11], thus the local temperature exceeds the glass transition temperature ( $1202 \text{ }^\circ\text{C}$ ) [12]. This can help to accelerate the melting of  $\text{SiO}_2$  glass.  $\text{SiO}_2$  melts then spreading out and when an adequate amount of  $\text{SiO}_2$  melts contacted with  $\text{Yb}_2\text{SiO}_5$ , they can transform the monosilicate into disilicate as following reaction:



Because  $\text{Yb}_2\text{Si}_2\text{O}_7$  has volume density larger than  $\text{Yb}_2\text{SiO}_5$ , and  $\text{SiO}_2$  has volume density double that of SiC [13], the disilicate product has larger volume than total volume loss of the silicon carbide and monosilicate reactants. In other words, this newly formed  $\text{Yb}_2\text{Si}_2\text{O}_7$  has the tendency to expand the hybrid's volume. Due to the dense structure of the hybrid, the expansion of  $\text{Yb}_2\text{Si}_2\text{O}_7$  in the direction away from the crack is very limited, and hence it has a tendency to expand towards the crack. The expanding direction of newly formed  $\text{Yb}_2\text{Si}_2\text{O}_7$  is illustrated by black arrows in Fig. 7. This volume expansion eventually heals the cracks.

#### 4.2. Strength's recovery and improvement

Figure 8 shows the bending strength measured from the hybrids. The bending strength of the hybrid without SiC is  $152 \text{ MPa}$ , which is comparable to reference value ( $159 \text{ MPa}$ ) in [10]. The variation of

strength in as-sintered hybrids is also similar to that of hardness and fracture toughness, increasing gradually to maximum value at  $10 \text{ vol.}\%$  SiC addition, then declining at higher SiC content. In as-indented specimens, the strength was reduced by  $30 \sim 50\%$ , compared to that of as-sintered specimens. However, it is obvious that the strength of all SiC hybrids recovered after the annealing in air. Bending strength of the hybrid dispersed with  $5 \text{ vol.}\%$  SiC recovered to the virgin value ( $152 \text{ MPa}$ ). In the hybrids with SiC content greater than or equal to  $10 \text{ vol.}\%$  the healing effect was even more impressive, in which healed specimens show strengths higher than the virgin value. The strength increments in  $10 \text{ vol.}\%$  and  $20 \text{ vol.}\%$  SiC hybrids were  $34 \text{ MPa}$  and  $62 \text{ MPa}$ . This improvement is considered to have relation to the residual compressive stress around the indentation caused by heat-treatment [14]. The modest strength recovery in the specimen annealed in Ar (from  $123$  to  $146 \text{ MPa}$ ) is not owing to the healing effect, but to the toughness improvement by the SiC particles in the hybrid [15].

Figure 9 shows the optical and SEM images after the bending test of as-sintered, as-indented, annealed in air (or Ar) of specimens with  $10 \text{ vol.}\%$  SiC. In the four-point bending test, the fracture may not develop through the center of the specimen, but cross the weakest points located somewhere between the two loading pins. For the specimen annealed in Ar, the fracture occurred at the center and developed through the indentation cracks (see Fig. 9b). This suggests that the crack-healing was ineffective in this case and the indentation is still the most severe

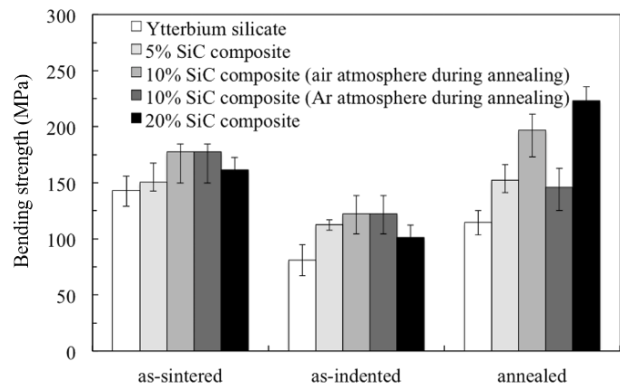


Fig. 8 Bending strength of as-sintered, as-indented, and annealed hybrids (annealing condition is  $1250 \text{ }^\circ\text{C}$ ,  $2 \text{ h}$ , in air or Ar)

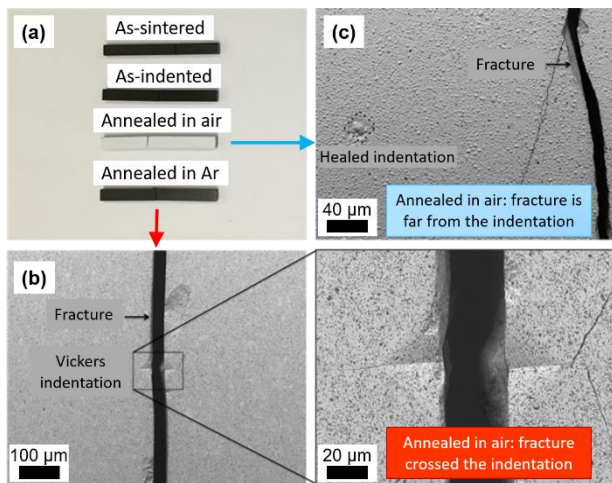


Fig. 9 (a) Optical images of fractured specimens; (b) and (c) SEM images of fracture specimens annealed in air and Ar

defect on the surface. For the specimen annealed in air (for 2 h), the fracture was developed at a site distant from the indentation (Fig. 9c), indicating that the indentation cracks have been healed completely.

#### 4.3. Recycling of healing agent:

Figure 10 shows SEM observation and composition analysis of a hybrid with 10 vol.% SiC, after thermal treatment in water vapor at 800 °C for 1 h. It should be noticed that prior to thermal treatment, this hybrid was annealed in air for 2 h, and most of  $\text{Yb}_2\text{SiO}_5$  (light gray domains) were transformed to  $\text{Yb}_2\text{Si}_2\text{O}_7$  (dark gray domains), as shown in Fig. 6b. However, in Fig. 10, we can see many light gray domains which may correspond to monosilicate. This suggests that the thermal treatment in water vapor has some effect on reversing  $\text{Yb}_2\text{Si}_2\text{O}_7$  to  $\text{Yb}_2\text{SiO}_5$ , as we expected. The mapping results for the whole observed area reveal that Yb:Si ratio is 18:23. Not only  $\text{Yb}_2\text{Si}_2\text{O}_7$ , but also other phases ( $\text{Yb}_2\text{SiO}_5$ ,  $\text{SiO}_2$ , etc.) may contribute to this ratio. XRD analysis is being conducted to identify the compounds existing at the hybrid surface.

### 5. Summary and Perspective

In the present research, YYS hybrid materials were sintered by a solid state reaction and hot pressing method. Their self-crack healing ability was investigated in relations with parameters such as annealing atmosphere and healing agent content. The filling up of  $\text{SiO}_2$  glass into the crack and the volume expansion of newly-formed  $\text{Yb}_2\text{Si}_2\text{O}_7$  are the

two main phenomena determining the crack healing in these hybrids. The hybrid with 10 vol.% SiC showed the highest hardness and toughness, superior strength, which can be fully recovered and further enhance by self-crack healing ability.

Self-healing is a very important property of  $\text{Yb}_2\text{Si}_2\text{O}_7$ - $\text{Yb}_2\text{SiO}_5$ -SiC hybrid for EBC materials and other high-temperature components. In a real gas turbine system, EBC should retain this ability for thousands of operating hours of the turbine blades. For that reason, the hybrid must reobtain the healing agents, i.e. SiC and  $\text{Yb}_2\text{SiO}_5$ , after each cycle of crack-healing. The thermal treatment in water vapor has demonstrated that it can help to reverse  $\text{Yb}_2\text{Si}_2\text{O}_7$  back to  $\text{Yb}_2\text{SiO}_5$ , as a result we can expect a permanent self-crack healing ability for YYS. Further analyses are being conducted to confirm the effectiveness of this thermal treatment technique.

### Acknowledgments

A major part of this work was conducted at Extreme Energy-Density Research Institute, Nagaoka University and Technology, the previous institution of the first author. The authors are grateful to technicians at National Institute of Technology, Kushiro College and Japan Fine Ceramics Center for their assistance in SEM-EDS mapping analysis and water vapour heat treatment. This work was partly supported by Japan Society for the Promotion of Science (JSPS) KAKENHI Grant-in-Aid for Early-Career-Scientists Number 18K14086.

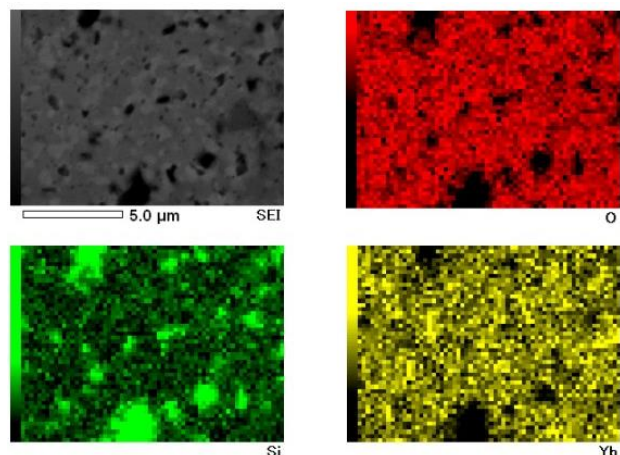


Fig. 10 SEM micrograph and EDS mapping results of the hybrid thermally treated in water vapor (red: O; green: Si; yellow: Yb).

## References

- [1] J.H. Perepezko, The hotter the engine, the better, *Science*. 326 (2009) 1068–1069.
- [2] I. Spitsberg, J. Steibel, Thermal and Environmental Barrier Coatings for SiC/SiC CMCs in Aircraft Engine Applications, *International Journal of Applied Ceramic*, 301 (2004) 291–301.
- [3] B.T. Richards, H.N.G. Wadley, Plasma spray deposition of tri-layer environmental barrier coatings, *Journal of the European Ceramic Society*. 34 (2014) 3069–3083.
- [4] K. Ando, K. Furusawa, K. Takahashi, S. Sato, Crack-healing ability of structural ceramics and a new methodology to guarantee the structural integrity using the ability and proof-test, *Journal of the European Ceramic Society*. 25 (2005) 549–558.
- [5] D. Maruoka, M. Nanko, Improved Crack Healing and High-Temperature Oxidation Resistance of Ni/Al<sub>2</sub>O<sub>3</sub> by Y or Si Doping, *Journal of the American Ceramic Society*. 99 (2016) 2451–2457.
- [6] Z. Chlup, P. Flasar, A. Kotoji, I. Dlouhy, Fracture behaviour of Al<sub>2</sub>O<sub>3</sub>/SiC nanocomposite ceramics after crack healing treatment, *Journal of the European Ceramic Society*. 28 (2008) 1073–1077.
- [7] S.T. Nguyen, T. Nakayama, H. Suematsu, T. Suzuki, L. He, H. Cho, K. Niihara, Strength improvement and purification of Yb<sub>2</sub>Si<sub>2</sub>O<sub>7</sub>-SiC nanocomposites by surface oxidation treatment, *Journal of the American Ceramic Society*. 100 (2017) 3122–3131.
- [8] S. Ueno, T. Ohji, H.-T. Lin, Recession behavior of Yb<sub>2</sub>Si<sub>2</sub>O<sub>7</sub> phase under high speed steam jet at high temperatures, *Corrosion Science*. 50 (2008) 178–182.
- [9] K. Niihara, A. Nakahira, T. Hirai, The effect of stoichiometry on mechanical properties of boron carbide, *Journal of the American Ceramic Society*. 67 (1984) C-13.
- [10] N. Al Nasiri, N. Patra, D. Horlait, D.D. Jayaseelan, W.E. Lee, Thermal Properties of Rare-Earth Monosilicates for EBC on Si-Based Ceramic Composites, *Journal of the American Ceramic Society*. 99 (2016) 589–596.
- [11] R. Frank, *Structural Ceramics Fundamentals and Case Studies*, (2009).
- [12] M. Ojovan, Glass formation in amorphous SiO<sub>2</sub> as a percolation phase transition in a system of network defects, *Journal of Experimental and Theoretical Physics Letters*. 79 (2004) 632–634.
- [13] P. Greil, Generic principles of crack-healing ceramics, *Journal of Advanced Ceramics*. 1 (2012) 249–267.
- [14] H.V. Pham, M. Nanko, W. Nakao, High-temperature Bending Strength of Self-Healing Ni/Al<sub>2</sub>O<sub>3</sub> Nanocomposites, *International Journal of Applied Ceramic Technology*. 13 (2016) 973–983.
- [15] K. Niihara, New Design Concept of Structural Ceramics, *Journal of the Ceramic Society of Japan*. 99 (1991) 974–982.